Biophysical Chemistry 253 (2019) 106226

Contents lists available at ScienceDirect

Biophysical Chemistry

journal homepage: www.elsevier.com/locate/biophyschem

The quaternary structure of insulin glargine and glulisine under formulation conditions

Norbert Nagel[a,*,1], Melissa A. Graewert[b,c,1], Mimi Gao[a], Winfried Heyse[a], Cy M. Jeffries[b], Dmitri Svergun[b,**], Harald Berchtold[a]

[a] Sanofi-Aventis Deutschland GmbH, R&D, Industriepark Höchst, 65926 Frankfurt, Germany
[b] European Molecular Biology Laboratory, Hamburg Unit, c/o DESY, Notkestraße 85, 22603 Hamburg, Germany
[c] BioSAXS GmbH c/o DESY, Notkestraße 85, 22603 Hamburg, Germany

HIGHLIGHTS

- In marketed formulations, insulin glulisine and glargine do not appear to consist of pure hexamers.
- Insulin glulisine is present as hexamers with significant fractions of monomers and dodecamers under formulation conditions.
- Dilution studies reveal a dissociation of the hexamers and dodecamers into monomers for insulin glulisine.
- Insulin glargine in Lantus and Toujeo demonstrates a hexamer-dimer equilibrium, which is maintained upon dilution with water.

GRAPHICAL ABSTRACT

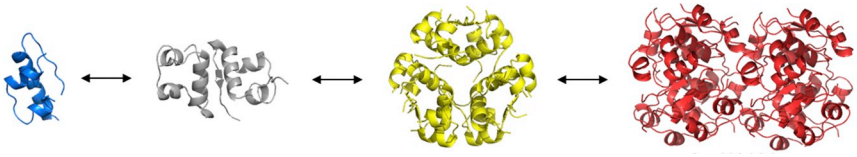

ARTICLE INFO

Keywords:
Insulin
Glargine
Glulisine
Quaternary structure
SAXS

ABSTRACT

The quaternary structures of insulin glargine and glulisine under formulation conditions and upon dilution using placebo or water were investigated using synchrotron small-angle X-ray scattering. Our results revealed that insulin glulisine in Apidra® is predominantly hexameric in solution with significant fractions of dodecamers and monomers. Upon dilution with placebo, this equilibrium shifts towards monomers. Insulin glargine in Lantus® and Toujeo® is present in a stable hexamer/dimer equilibrium, which is hardly affected by dilution with water down to 1 mg/ml insulin concentration. The results provide exclusive insight into the quaternary structure and thus the association/dissociation properties of the two insulin analogues in marketed formulations.

1. Introduction

Insulin is a pancreatic hormone that regulates normal blood glucose levels by facilitating cellular glucose uptake, regulating carbohydrate, lipid and protein metabolism. In 1952, human insulin was identified as a small protein consisting of chain A (21 amino acid residues) and chain B (30 amino acid residues) linked by two disulfide bonds. Since obesity and diabetes have reached epidemic severity, the continuous development and large-scale production of pharmaceutical insulin and insulin analogues to treat chronic hyperglycemia have become indispensable [1,2]. To mimic the physiological secretion of pancreatic β-cells under fasting and prandial conditions, different rapid- and long-acting insulin

* Corresponding author at: Sanofi-Aventis Deutschland GmbH, Industriepark Höchst, 65926 Frankfurt, Germany.
** Corresponding author.
E-mail addresses: norbert.nagel@sanofi.com (N. Nagel), svergun@embl-hamburg.de (D. Svergun).
[1] Equally contributed.

https://doi.org/10.1016/j.bpc.2019.106226
Received 10 April 2019; Received in revised form 18 June 2019; Accepted 10 July 2019
Available online 11 July 2019
0301-4622/

preparations were developed [1]. As the biologically active, circulating form of insulin is monomeric, but highly physico-chemically unstable, exogenous insulins are formulated as compact oligomers (mainly hexamers) or even in a crystalline state to ensure sufficient shelf life of the drug product. Therefore, knowing the quaternary structure of insulin and insulin analogues under pharmaceutical formulation conditions is important for improving the physical and chemical stability [3–7] of the drug product as well as for fine-tuning the absorption kinetics upon subcutaneous injection [8,9].

For some decades, it has been known that human, porcine and bovine insulins exhibit a similar and very complex association pattern in the crystalline state as well as in solution [10–14]. Among the prominent factors influencing the association state are the presence of zinc ions and phenolic compounds such as phenol or meta-cresol, the ionic strength of the solution, and the insulin concentration. In solution, at low pH (≤ 3) and in the absence of Zn^{2+} and phenolic compounds, naturally occurring insulin is present as monomers and/or dimers [10,15]. In addition, dimers have been observed at high pH and low zinc concentration, while around neutral pH different types of hexamers can form depending on the zinc concentration, the ionic strength and the presence or absence of phenolic compounds [10].

Insulin analogues are structurally modified to exhibit either faster and shorter or prolonged PK/PD (pharmacokinetics/pharmacodynamics) profiles for improved control of (post-)prandial and basal blood glucose levels while retaining the physiological insulin action (Fig. 1). As hexameric human insulin has to dissociate before absorption into the circulation occurs, certain amino acids are replaced in rapid-acting insulin analogues (B28 in insulin aspart, B28 and B29 in insulin lispro, B3 and B29 in insulin glulisine) to reduce the tendency of self-association allowing a rapid absorption without affecting the insulin-receptor kinetics [16]. After subcutaneous injection and upon dilution with interstitial fluid (twofold dilution after injection is expected) [17], the non-covalent oligomers of rapid-acting insulin analogues dissociate more rapidly into smaller species which are much faster absorbed than the oligomers [17,18]. In vitro dissociation kinetics of human insulin and fast acting insulin analogues upon dilution of the pharmaceutical formulation with an excess of PBS (1:20), as a test system, illustrate the concept and demonstrate the general differences of dissociation properties between such insulins (Fig. 2) [19]. While human insulin in a Zn^{2+} containing formulation remains almost completely hexameric (Insuman Rapid®, gray in Fig. 2), insulin aspart (in the Novorapid® formulation, blue in Fig. 2) and insulin lispro (in the Humalog® formulation, red in Fig. 2) dissociate into monomers within about 20 min. Insulin glulisine (in the Apidra® formulation, green in Fig. 2) dissociates even instantaneously under these conditions, triggered not only by the amino acid replacements, but also by the absence of the Zn^{2+} ions stabilizing the insulin hexamer, which are present in Humalog® and

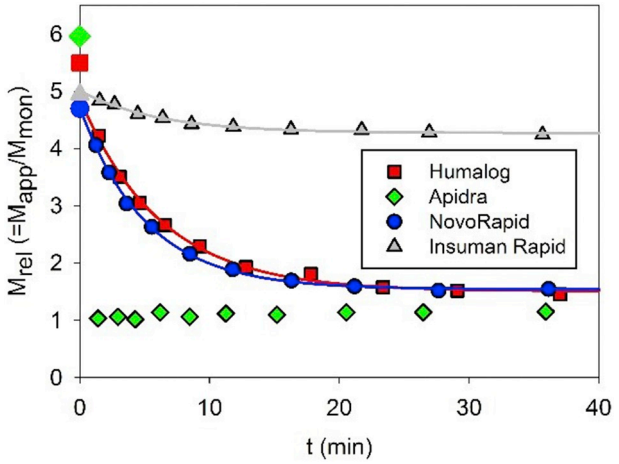

Fig. 2. Dissociation kinetics of non-covalent oligomers of human insulin and fast-acting insulin analogues upon a 20-fold dilution of the pharmaceutical formulation with PBS (phosphate buffer saline). The y axis represents the average molecular mass of the observed oligomer species relative to the monomer and the x axis the time in minutes upon dilution in PBS (from [19]).

Novorapid®. However, this large difference in dissociation rate between glulisine and the other insulins translates only to a lesser extent into clinical PK/PD profiles [20–22]. An explanation for this will be given in the Discussion section.

In contrast, to prolong the PK/PD profile of insulin for basal need, different strategies are known. In case of insulin glargine, two arginine residues are added to the C-terminus of the B-chain and AsnA21 is replaced by Gly (Fig. 1). This replacement increases the chemical stability by avoiding deamidation of AsnA21, which is an issue especially at low pH [5]. The two Arg residues shift the isoelectric point from pH 5.5 to pH 6.7. Furthermore, the modifications optimize the packing density of insulin hexamers [1,23]. Insulin glargine is formulated at pH 4.0, where it is soluble. After subcutaneous injection and mixing with interstitial fluid (pH 7.4), insulin glargine precipitates and the slow dissolution of insulin glargine from this subcutaneous depot together with the increased insulin glargine hexamer stability are the main reasons for the prolonged PK/PD profile [1]. It has been previously assumed that the precipitate is microcrystalline [1], which could not be confirmed by analytical investigations of insulin glargine precipitates obtained in vitro and in vivo, however (Sanofi unpublished results). Upon dissolution from the subcutaneous depot, insulin glargine undergoes an enzymatic removal of the basic arginine pair and the resulting metabolite (GlyA21 human insulin) is the main active component, while there is virtually no parent glargine circulating in the plasma [24].

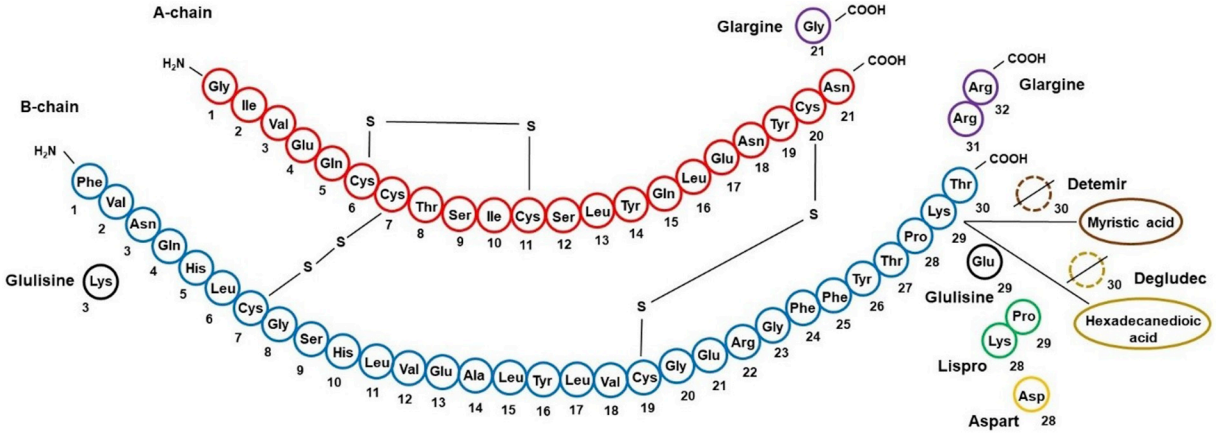

Fig. 1. Primary structure of human insulin and modifications in pharmaceutical insulin analogues.

Alternatively, the attachment of a fatty acid to the C-terminal region of the B-chain as in detemir and degludec prolongs the action of insulin by improving its strong self-association and binding to albumin in the blood (Fig. 1) [8]. In this approach, the insulin depot is not localized solely to the subcutis, but also comprises the plasma. In addition, insulin degludec self-assembles in filament-like complexes (multi-hexamers) upon depletion of phenol after subcutaneous injection, which may also contribute to the prolonged action [8].

However, compared to native insulin, its analogues are assumed to exhibit similar self-association patterns in formulations as long as just a few amino acids [1,2] are replaced or added, but are barely structurally characterized. A recent systematic ultracentrifugation analysis revealed that the hexameric state might not be the exclusive quaternary structure for many insulin analogues under formulation conditions [25,26].

In this publication, we present quaternary structure analysis for the two Sanofi insulins glulisine (Apidra®) and glargine (Lantus® and Toujeo®) in their respective pharmaceutical formulations obtained from synchrotron small-angle X-ray scattering (SAXS). We show that Apidra® primarily consists of hexamers with a significant fraction of monomers and dodecamers, which partially dissociate into monomers upon dilution with placebo. In the formulation conditions of Lantus® and Toujeo® (insulin glargine), the drug substance seems to be in a more stable hexamer-dimer equilibrium with only trace amounts of dodecamers. The results are compared with published quaternary structure information on human insulin and pharmaceutical insulin analogues and their implications are discussed.

2. Materials and methods

2.1. Materials

Apidra®, Lantus® and Toujeo® drug product solutions were taken from commercial material contained in cartridges and with shelf-life. The composition of the drug product solutions is given in Tables 1–3.

2.2. Small angle X-ray scattering

Synchrotron radiation X-ray scattering data from drug product solutions were collected at the EMBL P12 beamline of the storage ring PETRA III (DESY, Hamburg, Germany) [27]. Images were collected using a photon counting Pilatus-2 M detector at a sample to detector distance of 3.1 m and a wavelength (λ) of 0.12 nm covering the range of momentum transfer (s) $0.15 < s < 5\,\mathrm{nm}^{-1}$; with $s = 4\pi\sin\theta/\lambda$, where 2θ is the scattering angle). The drug product solutions were measured at the concentration as in the formulations, i.e. 10.91 mg/ml for Toujeo®, 3.64 mg/ml for Lantus® and 3.49 mg/ml for Apidra®. To assess the behavior upon dilution, the formulation was either diluted with placebo (formulation without drug substance) or double distilled water. A continuous flow cell capillary was used to reduce radiation damage. The latter was monitored by collecting 20 successive 50 ms exposures, comparing the frames, and discarding those displaying significant alterations.

In general, the respective placebos (formulations without drug substance) were suitable for background subtraction, especially for Apidra®. For Lantus® and Toujeo®, however, slight miss-matches were detected. This can be explained by the presence of zinc ions in the insulin glargine formulations that are added to influence the association state. Once these bind to the drug substance, and are thus removed from the excessive solvent, the electron density contrast of the solvent is reduced leading to an over-subtraction of the background scattering. Another effect of zinc ions is seen in the increase of radiation sensitivity of Lantus®. The earlier onset of radiation induced alterations leads to a decreased exposure duration, and thus, observed decrease in signal to noise ratio compared to Apidra® as scattering frames with traces of radiation damage are discarded. Nevertheless, suitable scattering curves could be obtained and used for further analysis.

Table 1
Composition of Apidra® per ml.

Insulin Glulisine®	3.49 mg
Sodium chloride	5.00 mg
m-Cresol	3.15 mg
Trometamol	6.00 mg
Polysorbate 20	0.01 mg
Water for injection	q.s. 1.00 ml
pH value	7.3

Table 2
Composition of Lantus® per ml.

Insulin Glargine®	3.64 mg
Zinc chloride	30 µg
m-Cresol	2.7 mg
Glycerol 85%	20 mg
Sodium hydroxide	q.s. to pH 4.0
Hydrochloric acid	q.s. to pH 4.0
Water for injection	q.s. to 1 ml

Table 3
Composition of Toujeo® per ml.

Insulin Glargine®	10.91 mg
Zinc chloride	0.19 mg
m-Cresol	2.7 mg
Glycerol 85%	20 mg
Sodium hydroxide	q.s. to pH 4.0
Hydrochloric acid	q.s. to pH 4.0
Water for injection	q.s. to 1 ml

The data were normalized to the intensity of the transmitted beam and radially averaged; the scattering of the placebo without drug substance (or ddH_2O) was subtracted and the difference curves were scaled for solute concentration. The forward scattering $I(0)$, the radius of gyration (R_g) along with the probability distribution of the particle distances $P(r)$ and the maximal dimension (D_{max}) were computed using the automated SAXS data analysis pipeline SASFLOW [28].

The molecular masses (MM) were evaluated by comparison of the forward scattering with that from reference solutions of bovine serum albumin. In addition, various concentration-independent methods were applied utilizing empirical relationships between MM and several structural parameters obtained directly from the data [29]. These approaches utilized the datporod [30], datmow [31], and datvc [32] modules of the ATSAS 2.8.3 package. In the datporod method, the excluded protein volume in $Å^3$ calculated from the Porod invariant [30] is divided by 1.6 to yield the MM estimate in Da. MoW, first implemented by Fischer et al. [31], also uses the scattering invariant and a fixed range of pre-defined values of s_{max} as well as empirical correction factors. The obtained volume is multiplied by the average mass density of proteins ($0.83 \times 10^3\,\mathrm{kDa\,Å}^{-3}$). Datvc is based on the observed relation between V_c^2 (squared volume of correlation) and R_g [32]. Additionally, a Bayesian inference approach takes the individual methods into account and reports MM estimates together with a credibility interval [29].

CRYSOL [33] was used to calculate the scattering profiles from the atomic coordinates of the available insulin structures (in house models as well as models from the Protein Data Bank (PDB [34]) and compare them with the experimental data.

To quantitatively characterize mixtures of different oligomeric species, the program OLIGOMER [35] was used, which fits the observed experimental data by a weighted combination of the theoretical scattering curves (form factors) from different quaternary structures. For insulin glargine, the final modelling was based on the biological assembly observed in the rhombohedral form of the m-cresol/insulin R6 hexamer (PDB entry 1ev3.pdb), which yielded the best agreement with the experimental data. For insulin glulisine a model developed in-house

was used. The arrangement of hexamers in the insulin dodecamer was taken as in the PDB entry 3 W80.

The graphical representations of the models were generated using PyMOL. (The PyMOL Molecular Graphics System, Version 2.0 Schrödinger, LLC.)

The experimental data and models are deposited in SASBDB [36] (https://www.sasbdb.org/) with the accession codes SASDF94, SASDFA4, SASDFB4.

3. Results

3.1. Insulins glargine (Lantus®) and glulisine (Apidra®) differ in apparent molar mass despite being formulated at the same concentration

In the development of insulin formulations, knowledge on the quaternary state of the hormone and its analogues is crucial to account for the physical and chemical stability of the drug substance as well as to determine ways for further improvement. Here, we set out to understand the composition of the insulin analogues under formulation conditions. Solution SAXS is an ideal method for this as the technique is not hampered by restrictive sample requirements, and the drug substances can be evaluated directly in the formulation without any further sample manipulation.

The synchrotron SAXS data were collected (Table 4: SAXS data) directly on the formulations and the scattering from respective placebos (formulations without drug substance) was subtracted as described in Methods. Fig. 3 displays the comparison of Apidra® with Lantus® both formulated at similar concentrations, which correspond to U100

Table 4
Data collection and SAXS-derived parameters.

Data collection parameters			
Radiation source	Petra III (DESY, Hamburg, Germany)		
Beamline	EMBL P12		
Detector	Pilatus 2 M, Pilatus 6 M		
Beam geometry (mm^2)	0.2 × 0.12		
Wavelength (Å)	1.24		
Sample-detector distance (m)	3.1		
s range (nm^{-1})	0.002–0.45		
Exposure time (s)	0.045		
Temperature (°C)	20		
Overall parameters	Apidra®	Lantus®	Toujeo®
Concentration range (mg/ml)	0.87–3.49	3.64	1–10.91
R_g from Guinier approximation (Å)	23.1 ± 0.2	17.8 ± 0.6	18.0 ± 1.0
R_g from PDDF (Å)	23.3 ± 0.2	18.3 ± 0.6	18.0 ± 1.0
D_{MAX} (Å)	75 ± 6	53 ± 4	62 ± 5
Molecular weight from forward scattering I(0), (kDa)	34 ± 3	35 ± 3	Na.
Molecular weight from excluded volume (kDa)	33 ± 3	28 ± 3	na.
Molecular weight from DATMOV, (kDa)	35 ± 3	35 ± 3	na.
Molecular weight from volume of correlation (kDa)	35 ± 3	26 ± 3	na.
Bayesian Credibility interval; (kDa, probability)	33–37 kD (94%)	30–33 kD (91%)	na.
Molecular weight from sequence (monomer, kDa)	5.8	6.1	6.1
Software employed			
Primary data reduction	SASFLOW		
Data processing	PRIMUS		
Calculation and comparison of scattering data	CRYSOL		
Mixtures modelling	OLIGOMER		
SASBDB accession code	SASDF94	SASDFB4	SASDFB4

Temporary links:
https://www.sasbdb.org/data/SASDF94/5jm7b16yjy/.
https://www.sasbdb.org/data/SASDFA4/qghaknhme8/.
https://www.sasbdb.org/data/SASDFB4/6ule5s2wha/.

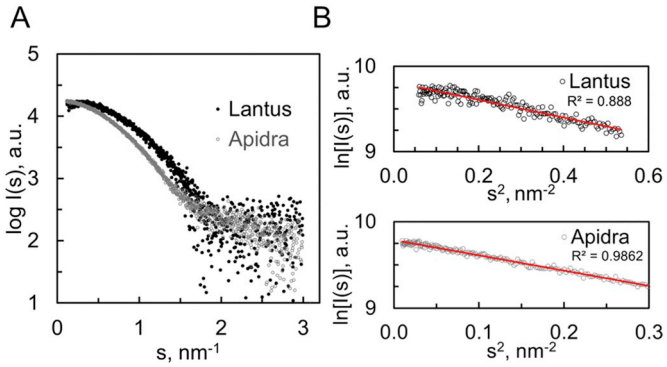

Fig. 3. Experimental scattering curves of insulin glulisine in Apidra® (gray) and insulin glargine in Lantus® (black). A, scattering profiles presented as log I(s). B, Guinier plots and linear regression (solid line) for evaluation of structure factor, R-squared values are indicated.

($c_{1Apidra}$ = 3.49 mg/ml and $c_{1Lantus}$ = 3.64 mg/ml). Despite only minor variations in the primary structure (Fig. 1), the solution scattering data from Apidra® and Lantus® show significant differences (Fig. 3). First, the interparticle interference effects are much stronger in the Lantus® formulation as revealed by a down-ward bend of its scattering profile at low angles. For Apidra®, the linear Guinier plot of the data at very low angles (ln$I(s)$ vs s^2, $s^2 < 0.3$ nm^{-2}, with the R-squared value R^2 = 0.986 (Fig. 3B, bottom panel) indicates that the complex is isotropic and neither affected by self-association (aggregation) nor repulsive interparticle interference effects. The Guinier plot of Lantus®, on the other hand, is non-linear at very low angles, ln$I(s)$ vs s^2, $s^2 < 0.5$ nm^{-2}, R^2 = 0.888 (Fig. 3B, top panel) with a negative curvature suggesting a repulsion between the scattering objects. This repulsion is a desired feature of the drug to prevent further association and undesired aggregation. This prolongs the shelf-life of insulin glargine and offers the possibility to increase its concentration. Note that the effect is yet stronger for Toujeo® (U300), as it will be discussed below. Second, although the average molecular mass (MM, Table 4) estimates derived from the scattering profiles of the formulated insulin homologues are similar with Bayesian credibility intervals of 33–37 kDa for Apidra® and 30–33 kDa for Lantus®, the faster decay of the Apidra® curve suggests that larger species are present in the formulation (see detailed analysis below). Interestingly, the apparent MM estimates are close to the expected MM of hexameric species (6 × 5.8 kDa ~ 35 kDa) suggesting that both formulations contain mainly hexamers. However, the subsequent analysis demonstrates that these formulations are heterogeneous solutions containing equilibrium mixtures of various oligomeric states.

3.2. Concentration-dependent mixture composition of insulin glulisine (Apidra®) and the presence of larger oligomeric species

To further analyze the oligomeric composition of the insulin glulisine, SAXS data were collected from a range of concentrations by diluting the formulation with placebo. Fig. 4A displays the scattering curves collected at concentrations c_1 (3.49 mg/ml), $c_{0.5}$ (1.74 mg/ml) and $c_{0.25}$ (0.87 mg/ml). The curves as well as the model-free parameters derived from them (Table 4) are in line with a concentration-dependent dissociation of the solute. To quantify this, we performed a mixture analysis of the scattering profiles with the program OLIGOMER [35], which fits the experimental data by linear combinations of the scattering curves computed from different oligomeric states. Initially, we tried to fit the data solely with hexamers, dimers and monomers; however the fits (blue lines) displayed noticeable systematic deviations indicating that higher species are present. The fits are significantly improved when allowing for the presence of dodecamers as illustrated in Fig. 4B and Table 5. On the other hand, the presence of dimers was

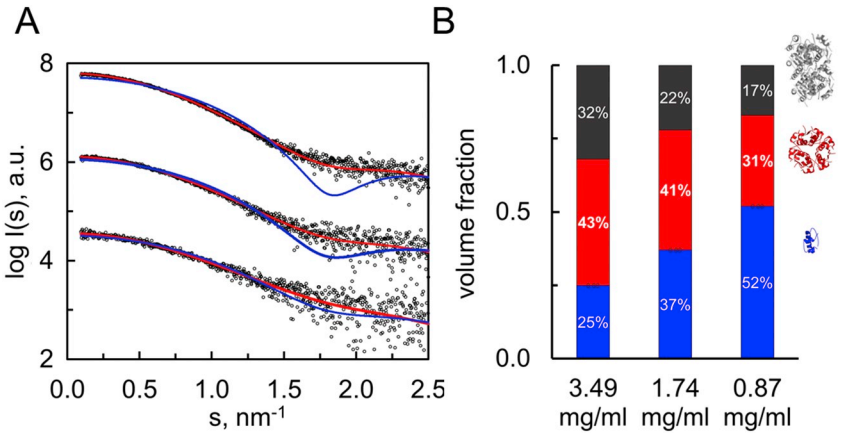

Fig. 4. Analysis of oligomeric composition of Apidra® at different concentrations. A, scattering profiles collected at c_1 = 3.49 mg/ml (top curve), at $c_{0.5}$ = 1.74 mg/ml (middle curve) and $c_{0.25}$ = 0.87 mg/ml (bottom curve); blue and red fits were obtained without and with the inclusion of dodecamers, respectively. For better visibility, the profiles and fits are shifted along the vertical axis. B, Stacked column diagram of the distribution of different oligomeric states displayed at the right as cartoons. Dodecamers, gray; hexamers, red; monomers blue.

Table 5
Concentration-dependent oligomeric composition of Apidra®.

Concentration	χ^2	Monomers	Dimers	Hexamers	Dodecamers
3.49 mg/ml*	1.08	25%	0%	43%	32%
1.74 mg/ml*	1.01	37%	0%	41%	22%
0.87 mg/ml*	0.97	56%	0%	31%	13%
3.49 mg/ml**	9.91	0%	0%	100%	–
1.74 mg/ml**	2.4	7%	0%	93%	–
0.87 mg/ml**	1.14	43%	0%	57%	–

Parameters obtained from fitting the SAXS data with (*) and without (**) dodecamers in the mixtures.

not required to fit the experimental data, and their volume fraction was always essentially zero. From this, we conclude that the larger complexes (hexamers and even dodecamers), present at the highest concentration, directly dissociate into monomers upon dilution in the Apidra® formulation. The specific amino acid replacements as well as the absence of the insulin hexamer stabilizing Zn^{2+} ions drive the equilibrium to the active monomeric state and are in agreement with the expected working mechanism for these rapid-acting insulin analogues. Most importantly, the volume fraction of the dodecamers decreases with dilution, so that their formation is reversible and should neither alter the medical relevant dosage of the drug substance, nor lead to the formation of potentially harmful aggregates. A recent publication [25] also reported three oligomeric species of insulin glulisine under formulation conditions based on analytical ultracentrifugation. The authors proposed the three species to be dimers, hexamers and dodecamers. To correlate our results with those reported in [25], we fitted the experimental Apidra® data assuming a mixture of dimers, hexamers and dodecamers, not allowing for monomers. In these fits the dimeric fraction was essentially replacing that of monomers and the fits were worse.

3.3. Repulsive and attractive interactions of insulin glargine (Lantus® and Toujeo®) at different concentrations

In both formulations, interparticle repulsions between the insulin oligomers exist, ensuring sufficient shelf-life by preventing further association and subsequent aggregation. In terms of a scattering experiment, the excluded volume effect resulting from the repulsion leads to a downward trend in the scattering profiles at low *s* (Fig. 5A). Here, the effect is obviously stronger for Toujeo®, formulated at U300 (10.91 mg/ml, black curve) than Lantus® which is formulated at U100 (3.64 mg/ml, blue curve). Overall, the curves overlay well indicating that the two samples possess a similar structural arrangement as well as oligomeric composition. Dilution experiments for the systematic analysis of insulin glargine were more challenging than for insulin glulisine. On the one hand, the unbuffered state of the formulation is very sensitive to introduction of normally negligible amounts of residual cleaning solution and can lead to a shift in pH of such a magnitude that by passing its isoelectric point, aggregates are formed. This is reminiscent of the working mechanism of insulin glargine to act as a long-lasting insulin. This analogue has been designed to form an insoluble depot upon injection (i.e. upon dilution with interstitial fluid and pH shift). On the other hand, dilution also shifts the equilibrium between excess zinc and phenol molecules that are part of the formulation composition. This creates difficulties in obtaining scattering frames suitable for background subtraction. In addition, the presence of zinc also increases the sensitivity to radiation and thus limiting the length of exposure. After testing various solutions for dilution as well as background subtraction, we found the dilution with ddH_2O to be most suitable for keeping the glargine solutions well behaving and obtain interpretable scattering curves at lower concentrations. A 10-time dilution of Toujeo® in ddH_2O led to a pH change from 3.9 to 4.3. Scattering data from samples in which dilution did artificially lead to aggregation were discarded and those without traces of aggregate formation were averaged to have the data with sufficient signal. Data collected from a concentration series ranging from 1 mg/ml to 10.5 mg/ml were collected (Fig. 5). The curves vividly demonstrate the transition from repulsive interactions (downward bend) for Toujeo® in the original formulation to attractive interactions (upward bend) upon dilution to lower insulin concentrations, which might be a consequence of a pH shift during dilution. This observation is fully consistent with the fact that upon pH increase of the formulation, insulin glargine is prone to aggregate and precipitate. This reduced solubility upon pH shift accounts for its prolonged action. Although the interparticle interference effects were changed upon dilution, the samples showed consistent scattering over a wider range of concentrations. This suggests that both formulations, Toujeo® and Lantus®, comprise a similar structural arrangement, oligomeric composition as well as surface charge.

3.4. Oligomeric composition of insulin glargine (Toujeo®)

Based on the molar mass estimates, insulin glargine is mainly hexameric (Table 4). To address the structural organization of these hexamers, we screened the experimental curve against a large number of PDB models in a similar manner as described in [37]. All examined hexamer models failed to adequately fit the data, even the best fit obtained with the biological assembly described by the m-cresol/insulin R6 hexamer (1ev3.pdb), revealed a rather high discrepancy (χ^2 above 4).

To improve the fits equilibrium mixture analysis was performed. As described for Apidra®, the data was fitted by the program OLIGOMER allowing for different distribution of monomers, dimers, hexamers and dodecamers. For the two highest concentrations quantification of the oligomeric composition is not straightforward as the data is strongly

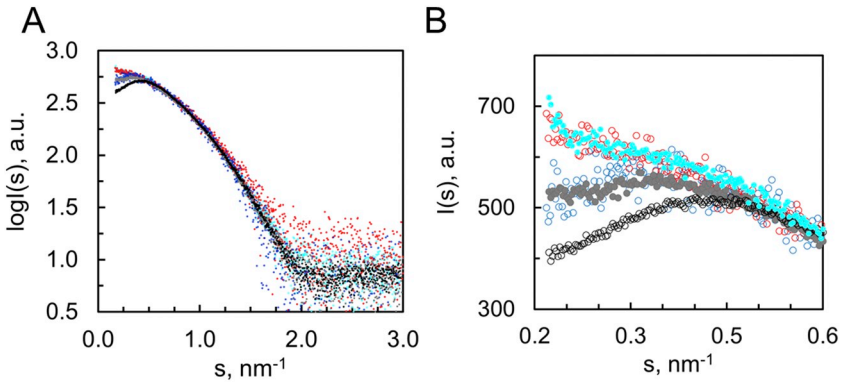

Fig. 5. Scattering profiles of insulin glargine under formulation conditions and dilutions thereof. Scattering profiles of Toujeo® U300 (10.91 mg/ml (black)), Lantus® U100 (3.64 mg/ml (blue), and Toujeo® at various dilutions in ddH_2O ($c_{0.5}$ = 5.54 mg/ml, light gray, filled; $c_{0.33}$ = 3.64 mg/ml, cyan, filled; $c_{0.01}$ = 1 mg/ml, red) are displayed (A), on log scale and (B), on linear scale (for smallest angles).

Table 6
Concentration-dependent oligomeric composition of *Toujeo®*.

Concentration	χ^2	Monomers	Dimers	Hexamers	Dodecamers
U300 10.9 mg/ml[a]	2.3	0%	47%	53%	–
5.54 mg/ml	3.7	0%	41%	59%	0%
3.64 mg/ml	1.27	0%	39%	57%	4%
1.0 mg/ml	1.03	0%	47%	50%	3%

[a] Note, only scattering data at $s > 0.5\,nm^{-1}$ was used for the fitting because due to the effect of interparticle interference.

influenced by the interparticle interactions. For undiluted Toujeo®, the fitting could only be performed for $s > 0.5\,nm^{-1}$. Very good fits were obtained with approximately 40% dimers in addition to hexamers. For lower concentrations a small volume fraction of dodecamers (≤4%) also improved the fit (Table 6; Fig. 6). The contribution to the scattering profile of this higher oligomeric species would most likely be "overshadowed" by the effect from the interparticle repulsion at higher concentrations and is thus not observable. Taken together, our results indicate for insulin glargine a stable hexamer-dimer distribution in both formulations as well as over a wider range of concentrations. Consistently, using dynamic light scattering (DLS) and analytical ultracentrifugation (AUC), Adams et al. reported that the oligomeric composition of both dosage strengths of insulin glargine is practically identical [25,26]. However, they assume that insulin glargine is purely or predominantly dimeric. Our results clearly indicate that glargine samples contain much larger oligomers than dimers. Even for the lowest solute concentration (1 mg/ml), an attempt to fit the glargine data with the computed scattering from the insulin dimer yielded a very poor fit with $\chi^2 = 5.0$, such that higher oligomers are indispensable to obtain agreement with the experimental data. A potential explanation for the observed discrepancy to the oligomer assessment reported in [25,26] could be an underestimation of the non-ideality of the insulin glargine formulations in AUC and DLS, as the repulsive interactions reported here enable a faster diffusion, potentially resulting in decreased apparent masses and hydrodynamic radii.

4. Discussion

We have investigated the quaternary structure of the two Sanofi insulins, glulisine (Apidra®) and glargine (Lantus® and Toujeo®) in their respective marketed formulations and the influence of dilution on the oligomeric composition. Synchrotron SAXS was our method of choice since it allows one to investigate the formulations at defined insulin concentrations without applying any kind of stress, which may influence the quaternary structure.

We showed that the three formulations are mainly hexameric insulins, but they also contain smaller and larger oligomeric species, in significant amounts. Apidra® displayed a concentration-dependent oligomerization equilibrium between monomers, hexamers and dodecamers. At U100, Apidra® is present largely as hexameric insulin with significant fractions of monomers and dodecamers, whereas the monomers become a dominating species at lower concentrations when diluting with the placebo. In contrast, Toujeo® and Lantus® appear to be present largely as a hexamer-dimer-system. Upon dilution with water the equilibrium remains nearly unchanged.

The above results further support our understanding of the mode of action of the investigated insulins and of the observed PK/PD profiles [20]. Upon subcutaneous injection of typical insulin doses, an initial dilution with interstitial fluid of approximately a factor of two can be expected [17]. The first step in the insulin absorption process following subcutaneous injection is mainly diffusion-controlled. Therefore, the association state of the insulin analogue in the formed subcutaneous depot will have a pronounced effect on the PK/PD profile. Larger insulin associates diffuse slower into subcutis regions of lower insulin concentration, where they can dissociate into smaller oligomers and finally monomers. Only the monomers can then, in the next absorption step easily enter the blood stream through the endothelium and become

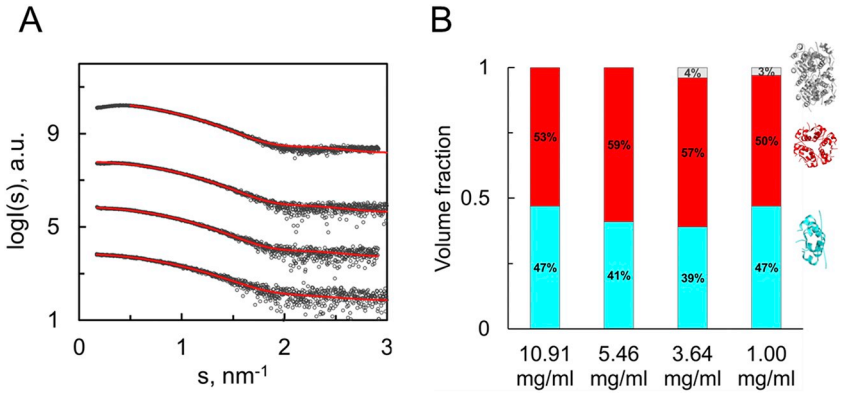

Fig. 6. Analysis of oligomeric composition of insulin glargine at different concentrations. A, scattering profiles collected at Toujeo® formulation concentration (10.91 mg/ml, top curve), $c_{0.5}$ = 5.45 mg/ml (second curve), $c_{0.33}$ = 3.56 mg/ml (third curve), and $c_{0.1}$ = 1 mg/ml (bottom). Experimental data is shown in black and fits are shown in red. B, Stacked column diagram of the distribution of different oligomeric states displayed at the right as cartoons. Dodecamers, gray; hexamers, red; dimers, cyan.

systemically available.

Glargine in Lantus® and Toujeo® is designed to have an isoelectric point of about 7.0 and thus forms very large associates upon subcutaneous injection and dilution with interstitial fluid. These large associates finally form a precipitate facilitating a delayed and prolonged absorption from the injection site. At a slightly acidic pH, as in the marketed formulations, glargine is fully soluble and present as a stable hexamer-dimer equilibrium as we found in this study. Recently, glargine dimers were reported by dynamic light scattering and analytical ultracentrifugation as well [26]. Further, the observed interparticle interference effects clearly revealed the propensity of insulin glargine for attractive interactions upon pH increase towards physiological pH, which is the required condition for precipitation. In contrast, insulin degludec (Tresiba®), another long-acting insulin, forms dodecamers (dihexamers) in marketed formulations and associates to multi-hexamers in linear arrays upon phenol/cresol depletion [38]. The quaternary structure of insulin analogues in formulations frequently differs from the oligomeric state in the subcutaneous tissue.

The situation for glulisine in Apidra® is different. Upon dilution with placebo, we show that the oligomeric state of the insulin analogue is significantly shifted to smaller oligomers (monomers), though still far away from being purely monomeric. However, under tested conditions glulisine hexamers have been shown to dissociate much faster compared to other fast-acting insulins [19]. Those observations are consistent with the fact that the exchange of asparagine at B3 for lysine induces slight steric and electrostatic repulsion between the monomer molecules thus facilitating a rapid dissociation into the active monomeric insulin upon dilution and depletion of ligands [20]. On the other site, the exchange at B29 for glutamic acid allows stabilization of the monomer realizing even a stable zinc-free formulation. In contrast, another strategy to accelerate hexamer dissociation in vivo is to introduce mutations impairing the dimer interface as done in insulin aspart and lispro. Interestingly, both strategies lead to similar clinical PK/PD profiles of the marketed fast acting insulins. In the subcutis immediately upon injection, the expected dilution (about 1:1 with interstitial fluid according to [17]) hardly changes the oligomeric equilibria of marketed fast acting insulins [19]. A potential approach to even faster-acting insulins could be to design an insulin analogue, which upon injection of a suitable formulation is purely or highly monomeric in the subcutaneous depot. Recent developments of faster acting insulins follow the approach to add novel excipients to formulations of an established insulin analogue, which facilitate insulin absorption [39–41]. These excipients (niacinamide, trepostinil) are known to be vascodilators, however, their exact mode of action is still subject of investigations and discussion.

In conclusion, we demonstrated that SAXS is a powerful tool to investigate quaternary structure and thus association/dissociation behaviors of insulin in formulations and upon dilutions. Our results further indicate that stable insulin formulations can be mixtures of different oligomeric states and are not necessarily pure hexamer solutions as previously believed.

Acknowledgements

MAG received support from iNEXT, grant number 653706, funded by the Horizon 2020 program of the European Union (PID: 2861).

References

[1] R. Hilgenfeld, G. Seipke, H. Berchtold, D.R. Owens, The evolution of insulin glargine and its continuing contribution to diabetes care, Drugs 74 (8) (2014) 911–927.
[2] G. Danaei, et al., National, regional, and global trends in fasting plasma glucose and diabetes prevalence since 1980: systematic analysis of health examination surveys and epidemiological studies with 370 country-years and 2·7 million participants, Lancet 378 (9785) (2011) 31–40.
[3] M. Groenning, S. Frokjaer, B. Vestergaard, Formation mechanism of insulin fibrils and structural aspects of the insulin fibrillation process, Curr. Protein Pept. Sci. 10 (5) (2009) 509–528.
[4] R.J. Woods, J. Alarcón, E. McVey, R.J. Pettis, Intrinsic fibrillation of fast-acting insulin analogs, J. Diabetes Sci. Technol. 6 (2) (2012) 265–276.
[5] J. Brange, L. Langkjaer, S. Havelund, A. Vølund, Chemical stability of insulin. 1. Hydrolytic degradation during storage of pharmaceutical preparations, Pharm. Res. 9 (6) (1992) 715–726.
[6] J. Brange, S. Havelund, P. Hougaard, Chemical stability of insulin. 2. Formation of higher molecular weight transformation products during storage of pharmaceutical preparations, Pharm. Res. 9 (6) (1992) 727–734.
[7] J. Brange, Stability of Insulin, Kluwer Academic Publishers, 1994.
[8] I. Jonassen, et al., Design of the novel protraction mechanism of insulin degludec, an ultra-long-acting basal insulin, Pharm. Res. 29 (8) (2012) 2104–2114.
[9] J. Brange, et al., Monomeric insulins obtained by protein engineering and their medical implications, Nature 333 (1988) 679.
[10] J. Brange, Galenics of Insulin, Springer, Berlin, 1987.
[11] J.J. Abel, Crystalline insulin, Proc. Natl. Acad. Sci. U. S. A. 12 (2) (1926) 132–136.
[12] D.A. Scott, A.M. Fisher, Crystalline insulin, Biochem. J. 29 (5) (1935) 1048–1054.
[13] K. Hallas-Møller, K. Petersen, J. Schlichtkrull, Crystalline and amorphous insulin-zinc compounds with prolonged action, Science 116 (3015) (1952) 394–398.
[14] T.L. Blundell, et al., Atomic positions in rhombohedral 2-zinc insulin crystals, Nature 231 (1971) 506.
[15] J.L. Whittingham, et al., Insulin at pH 2: structural analysis of the conditions promoting insulin fibre formation, J. Mol. Biol. 2836 (02) (2002) 479–490.
[16] J. Brange, D.R. Owens, S. Kang, A. Vølund, Monomeric insulins and their experimental and clinical implications, Diabetes Care 13 (9) (1990) 923–954.
[17] C.H. Rasmussen, et al., Insulin aspart pharmacokinetics: an assessment of its variability and underlying mechanisms, Eur. J. Pharm. Sci. 62 (2014) 65–75.
[18] T. Søeborg, C.H. Rasmussen, E. Mosekilde, M. Colding-Jørgensen, Absorption kinetics of insulin after subcutaneous administration, Eur. J. Pharm. Sci. 36 (1) (2009) 78–90.
[19] K. Gast, et al., Rapid-acting and human insulins: hexamer dissociation kinetics upon dilution of the pharmaceutical formulation, Pharm. Res. 34 (11) (2017) 2270–2286.
[20] R.H.A. Becker, Insulin Glulisine complementing basal insulins: a review of structure and activity, Diabetes Technol. Ther. 9 (1) (2007) 109–121.
[21] G.B. Bolli, et al., Comparative pharmacodynamic and pharmacokinetic characteristics of subcutaneous insulin glulisine and insulin aspart prior to a standard meal in obese subjects with type 2 diabetes, Diabetes. Obes. Metab. 13 (3) (2011) 251–257.
[22] T. Heise, et al., Insulin glulisine: a faster onset of action compared with insulin lispro, Diabetes. Obes. Metab. 9 (5) (2007) 746–753.
[23] H. Berchtold, R. Hilgenfeld, Binding of phenol to R6 insulin hexamers, Biopolymers 51 (2) (1999) 165–172.
[24] G.B. Bolli, et al., Plasma exposure to insulin glargine and its metabolites M1 and M2 after subcutaneous injection of therapeutic and supratherapeutic doses of glargine in subjects with type 1 diabetes, Diabetes Care 35 (12) (2012) 2626–2630.
[25] G.G. Adams, et al., Characterisation of insulin analogues therapeutically available to patients, PLoS One 13 (3) (2018) e0195010.
[26] G.G. Adams, et al., Glargine and degludec: solution behaviour of higher dose synthetic insulins, Sci. Rep. 7 (1) (2017) 7287.
[27] C.E. Blanchet, et al., Versatile sample environments and automation for biological solution X-ray scattering experiments at the P12 beamline (PETRA III, DESY), J. Appl. Crystallogr. 48 (2015) 431–443.
[28] D. Franke, A.G. Kikhney, D.I. Svergun, Automated acquisition and analysis of small angle X-ray scattering data, Nucl. Instrum. Methods Phys. Res. Sect. A Accel. Spectrom. Detect. Assoc. Equip. 689 (2012) 52–59.
[29] N.R. Hajizadeh, D. Franke, C.M. Jeffries, D.I. Svergun, Consensus Bayesian assessment of protein molecular mass from solution X-ray scattering data, Sci. Rep. 8 (1) (2018) 7204.
[30] M.V. Petoukhov, et al., New developments in the ATSAS program package for small-angle scattering data analysis, J. Appl. Crystallogr. 45 (2) (2012) 342–350.
[31] H. Fischer, M. de Oliveira Neto, H.B. Napolitano, I. Polikarpov, A.F. Craievich, Determination of the molecular weight of proteins in solution from a single small-angle X-ray scattering measurement on a relative scale, J. Appl. Crystallogr. 43 (1) (2010) 101–109.
[32] R.P. Rambo, J.A. Tainer, Accurate assessment of mass, models and resolution by small-angle scattering, Nature 496 (2013) 477.
[33] D. Svergun, C. Barberato, M.H.J. Koch, CRYSOL - a program to evaluate X-ray solution scattering of biological macromolecules from atomic coordinates, J. Appl. Crystallogr. 28 (6) (1995) 768–773.
[34] H.M. Berman, et al., The protein data bank, Nucleic Acids Res. 28 (1) (2000) 235–242.
[35] P.V. Konarev, V.V. Volkov, A.V. Sokolova, M.H.J. Koch, D.I. Svergun, PRIMUS: a windows PC-based system for small-angle scattering data analysis, J. Appl. Crystallogr. 36 (5) (2003) 1277–1282.
[36] E. Valentini, A.G. Kikhney, G. Previtali, C.M. Jeffries, D.I. Svergun, SASBDB, a repository for biological small-angle scattering data, Nucleic Acids Res. 43 (D1) (2015) D357–D363.
[37] M.H. Jensen, et al., Small angle X-ray scattering-based elucidation of the self-association mechanism of human insulin analogue LysB29(Nεω- carboxyheptadecanoyl) des(B30), Biochemistry 52 (2) (2013) 282–294.
[38] D.B. Steensgaard, et al., Ligand-controlled assembly of hexamers, dihexamers, and linear multihexamer structures by the engineered acylated insulin degludec, Biochemistry 52 (2) (2013) 295–309.
[39] A. Davis, J. Kuriakose, J.N. Clements, Faster insulin aspart: a new bolus option for diabetes mellitus, Clin. Pharmacokinet. (2018) 1–10.
[40] Christe ME, Hardy TA (2015) Patent WO 2015/171484 Al.
[41] T. Biester, O. Kordonouri, T. Danne, Pharmacological properties of faster-acting insulin Aspart, Curr. Diab. Rep. 17 (11) (2017) 1–6.